Transactions of the Materials Research Society of Japan 29[7] 3013-3016 (2004)

Microstructural Characterization and Shape Memory Effects of Ti-Nb-Al Alloys

Tomonari Inamura, Yusuke Fukui*, Hideki Hosoda†, Kenji Wakashima and Shuichi Miyazaki**

Precision and Intelligence Laboratory, Tokyo Institute of Technology, 4259 Nagatsuta, Midori, Yokohama, 226-8503, Japan
Fax:+81-45-924-5061, e-mail:inamura@pi.titech.ac.jp
*Graduate Student, Tokyo Institute of Technology, 4259 Nagatsuta, Midori, Yokohama, 226-8503, Japan
Fax:+81-45-924-5061, e-mail:fukui@ken.pi.titech.ac.jp
†Precision and Intelligence Laboratory, Tokyo Institute of Technology, 4259 Nagatsuta, Midori, Yokohama, 226-8503, Japan
Fax:+81-45-924-5057, e-mail:hosoda@pi.titech.ac.jp
**Institute of Materials Science, University of Tsukuba, Tennodai 1-1-1, Tsukuba, Ibaraki 305-8573, Japan
Fax:+81-298-53-5283, e-mail:miyazaki@ims.tsukuba.ac.jp

We have found that superelastic strain exceeding 4% can be obtained in the Ti-Nb-Al alloy sheets made by cold-rolling followed by a suitable thermomechanical treatment. However, the superelastic behavior of the sheets strongly depends on the loading direction relative to the rolling direction. Therefore, in order to understand the anisotropic superelastic behavior, phase constitution and microstructures were investigated by θ-2θ X-ray diffraction analysis (XRD), pole figure measurement, optical microscopy and transmission electron microscopy in the Ti-Nb-Al sheets. The nature of the anisotropic behavior in superelasticity in the material is discussed in terms of textures, based on the crystallography of the material and energy considerations.
Key words: superelasticity, thermomechanical treatment, texture, Ti-Nb-Al, pole figure

1. INTRODUCTION

Shape memory alloys (SMAs) are fascinating materials for biomedical applications. Although only Ti-Ni SMAs have been used for biomedical practical applications because of their superior shape memory properties as well as corrosion resistance, the probability of Ni hypersensitivity is pointed out for Ti-Ni SMAs. Therefore, in order to reduce the risk of toxicity of components, new biomedical SMAs consisting of nontoxic elements only, especially Ni-free, are required to replace Ti-Ni SMAs.

It has been reported that some Ti alloys have a martensitic transformation from β-phase (bcc) to α'-phase (hcp) or α"-phase (C-centered orthorhombic) by quenching [1-2].
Our group has systematically investigated new Ti-base SMAs [3-5]. It has been found that superelastic strain being more than 4% appears in the sheets of Ti-24mol%Nb-3mol%Al (termed 24Nb3Al hereafter) alloy made by cold-rolling of 99% followed by a solution-treatment at 1273K for 1.8ks [3]. The term '24Nb3Al-99%-ST' represents the specimen of 24Nb3Al which was cold-rolled to be 99% reduction in thickness followed by the solution-treatment (ST) hereafter. Figures 1(a) and 1(b) show cyclic loading-unloading curves of 24Nb3Al-99%-ST with the loading direction parallel to the rolling direction (RD) and the transverse direction (TD), respectively. Superelastic strain of about 4.7% appears along RD. However, only 2.2% of superelastic strain appears along TD. (For details of the mechanical properties, see Refer [3].)

This anisotropy in the superelastic behavior should be due to microstructures developed during the thermomechanical treatments. The objective of this study is to understand the nature of the anisotropic superelastic behavior of the sheets of 24Nb3Al, on the view point of microstructures.

2. EXPERIMENTAL PROCEDURES

The nominal compositions of Ti-18, 20, 22, 24mol%Nb-3mol%Al alloys were prepared in this study. These alloys are hereafter termed 18Nb3Al, 20Nb3Al, 22Nb3Al and

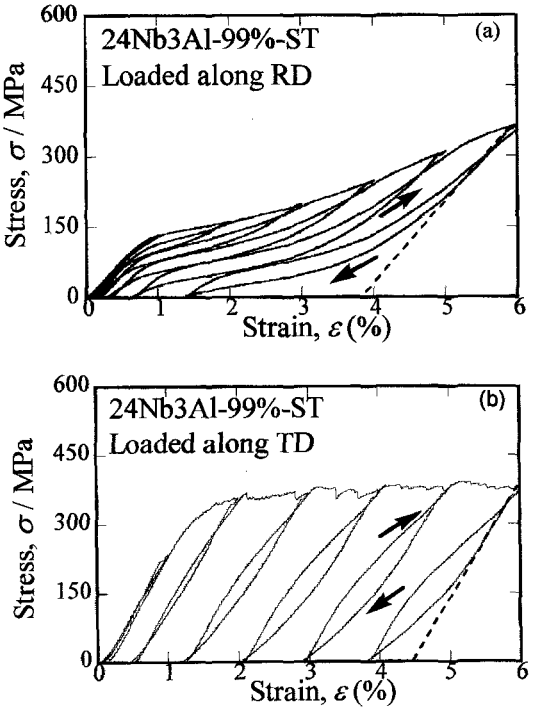

Figure 1: Cyclic loading-unloading curves of 24Nb3Al-99%-ST
(a) Loaded along RD, (b) Loaded along TD
Slope of the dashed lines indicates Young's modulus.

24Nb3Al, respectively. The alloys were prepared by Ar arc-melting method using high purity elemental Ti, Nb and Al. The ingots were homogenized at 1273K for 7.2 ks in vacuum, and then cold-rolled to be 99% reduction in thickness. The reduction corresponded to 0.1mm (99%) in thickness. As-rolled sheets were sealed in quartz tubes and then, a solution treatment at 1273K for 1.8 ks in vacuum was carried out. The sheets were quenched into water by breaking the quartz tubes in water.

The specimens for optical microscopy observations were mechanically polished by a diamond paste with 1μm in diameter followed by an electro-polishing and a chemical etching. Observations were carried out using a scanning laser microscope.

θ-2θ X-ray diffraction analysis (XRD) was conducted at RT with CuKα radiation using Philips X'pert-Pro system after removing damaged surface layer by an electro-polishing. Si was used as a standard element. X-ray pole figure measurements were also conducted with CuKα radiation using Philips X'pert-Pro MRD system equipped with a Ge-monochromater. Beam diameter was set to be 1 mm in the pole figure measurements.

Thin foils for transmission electron microscopy (TEM) observations were prepared using a twin-jet polishing technique. TEM observations were conducted using Philips CM200 operated at 200 kV.

3. RESULTS

3.1 Phase constitution

Figure 2 shows XRD patterns of 18Nb3Al, 20Nb3Al, 22Nb3Al and 24Nb3Al after the homogenization treatment. Since cold-rolled sheets were slightly buckled after the solution treatment, buckling degrades the accuracy of the determination of d-spacing. Therefore, phase constitution and the lattice parameters were also investigated using each alloy before the cold-rolling. The phases detected by XRD were summarized as follows;

18Nb3Al, 20Nb3Al : α"

22Nb3Al : α" + trace β

24Nb3Al : β

The apparent phase at RT was α" for 18Nb3Al and 20Nb3Al. Trace of β was detected in 22Nb3Al, in addition to α". 24Nb3Al was judged to be single phase of β at RT by XRD . 24Nb3Al-99%-ST was also found to be a single phase of β by XRD.

3.2 Lattice parameters of α"

For the convenience of the latter discussion, the lattice parameters of β and α" in 24Nb3Al are summarized here. Figure 3 shows the lattice parameters of the α" phase of each material, as a function of the Nb concentration (Note that the concentration of Al was fixed to be 3mol% in this study). The lattice parameters of α" in 24Nb3Al were determined by extrapolation of those of the other materials and calculated to be as follows.

a_β =0.3283nm

$a_{\alpha"}$=0.3197 nm, $b_{\alpha"}$ =0.4768 nm, $c_{\alpha"}$ =0.4619 nm

Where, the subscripts β and α" indicate β-austenite and α"-martensite, respectively. It should be noted that 24Nb3Al is the single phase of β at RT and the above lattice parameters of α" are the extrapolated values when the α" is stabilized at RT.

3.3 Substructures of 24Nb3Al-99%-ST

Optical microscopy observations revealed that the grains of 24Nb3Al-99%-ST were equiaxed with an averaged grain size of 74μm. No secondary phase was detected in optical microscopy.

TEM observations were conducted to obtain further information about the phase constitution and the substructure of the materials. Each β-grain had been severely deformed by the cold-rolling. However, dislocation density seemed to be drastically decreased in 24Nb3Al-99%-ST. Fine particles (a few nm in diameter) of ω-phase were detected entire grains of 24Nb3Al-99%-ST. These ω-particles must be 'quenched ω' which commonly

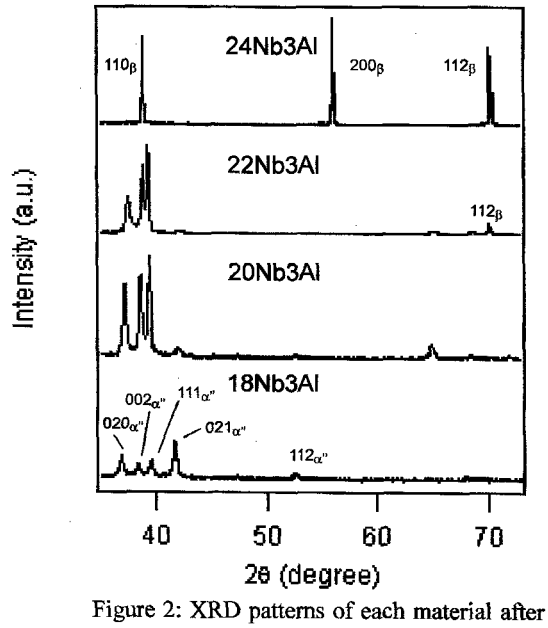

Figure 2: XRD patterns of each material after the homogenization treatment

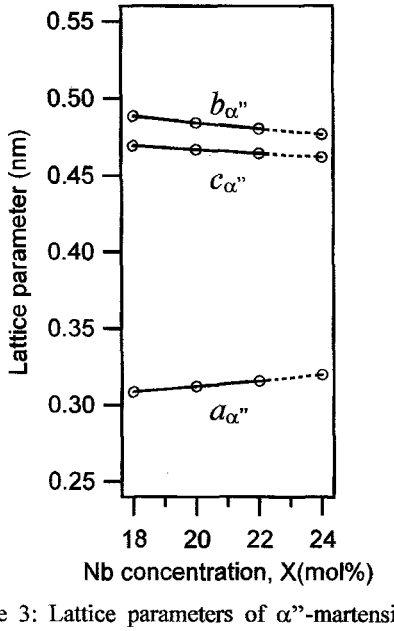

Figure 3: Lattice parameters of α"-martensite in Ti-Xmol%Nb-3mol%Al alloys (18<X<24)

exists in the Ti-Nb binary alloys [6]. The details of TEM and optical microscopy were reported in our previous study [7].

3.4 Texture of 24Nb3Al-99%-ST

X-ray pole figures were measured for 24Nb3Al-99%-ST using 110_β, 200_β and 112_β reflections. Figures 4(a) and 4(b) show 110_β and 200_β pole figures of 24Nb3Al-99%-ST. The RD is vertical to the paper, and the TD is parallel to the paper as shown in the figures. Dark and dense parts in the pole figures correspond to high intensity of diffracted X-ray. A recrystallization texture was clearly observed as shown in the pole figure. The background intensity was about 10 counts/sec and the maximum intensity was more than 40000 counts/sec. Therefore, the texture was deduced to be well developed. 112_β pole figures (not shown here) were also measured and it was found that the recrystallization texture of 24Nb3Al-99%-ST was $<110>_\beta\{112\}_\beta$.

Figure 4(c) shows a composite stereographic projection of the $<110>_\beta\{112\}_\beta$ recrystallization texture observed in 24Nb3Al-99%-ST. As seen in the stereoprojection, 24Nb3Al-99%-ST is mainly consisted with two β-variants (denoted by β_1 (the filled markers) and β_2 (the solid markers)) which are twin-related each other.

4 DISCISSION

4.1 The transformational strain

As experimentally confirmed, 24Nb3Al-99%-ST had a well developed texture. Therefore, α'' variant(s) preferentially induced under tension along RD (// $<110>_\beta$) should be different from that induced under tension along TD (// $<111>_\beta$). Following discussion is focused on (1) transformation strain of α'', (2) identification of the preferentially induced variant(s) under tension along RD and TD in the $<110>_\beta\{112\}_\beta$ texture and (3) resultant transformation strain along the loading direction.

Figure 5 shows Au-Cd type lattice correspondence [8]. This lattice correspondence was regarded as the most plausible one in this study and transformation strain was calculated based on the correspondence. Using the lattice parameters of a_β =0.3283nm, $a_{\alpha''}$=0.3197 nm, $b_{\alpha''}$ =0.4768 nm and $c_{\alpha''}$ =0.4619 nm, a principal strain of the transformation can be calculated as follows for a α''-variant.

$$\varepsilon^* = \begin{pmatrix} -0.0263 & 0 & 0 \\ 0 & -0.0052 & 0 \\ 0 & 0 & 0.0270 \end{pmatrix} \quad (1)$$

The transformation strain in Eq(1) can be expressed as follows referred to the bcc lattice coordinate system.

$$\varepsilon_1^* = \begin{pmatrix} -0.0263 & 0 & 0 \\ 0 & 0.0109 & -0.0161 \\ 0 & -0.0161 & 0.0109 \end{pmatrix} \quad (2)$$

It can be deduced from the lattice correspondence that there are six lattice correspondence variants for the transformation. The transformation strains of each variant are calculated by a suitable coordinate transformation of ε_1^*.

4.2 Preferred variant

When the transformation was induced by an external stress, the variants which reduce potential energy of the external stress are preferentially formed [9]. Then, interaction energy U was calculated to evaluate which variant is preferentially induced under tension along RD and TD. According to Mura [10], interaction energy U is defined as follows, for unit volume of the material with the

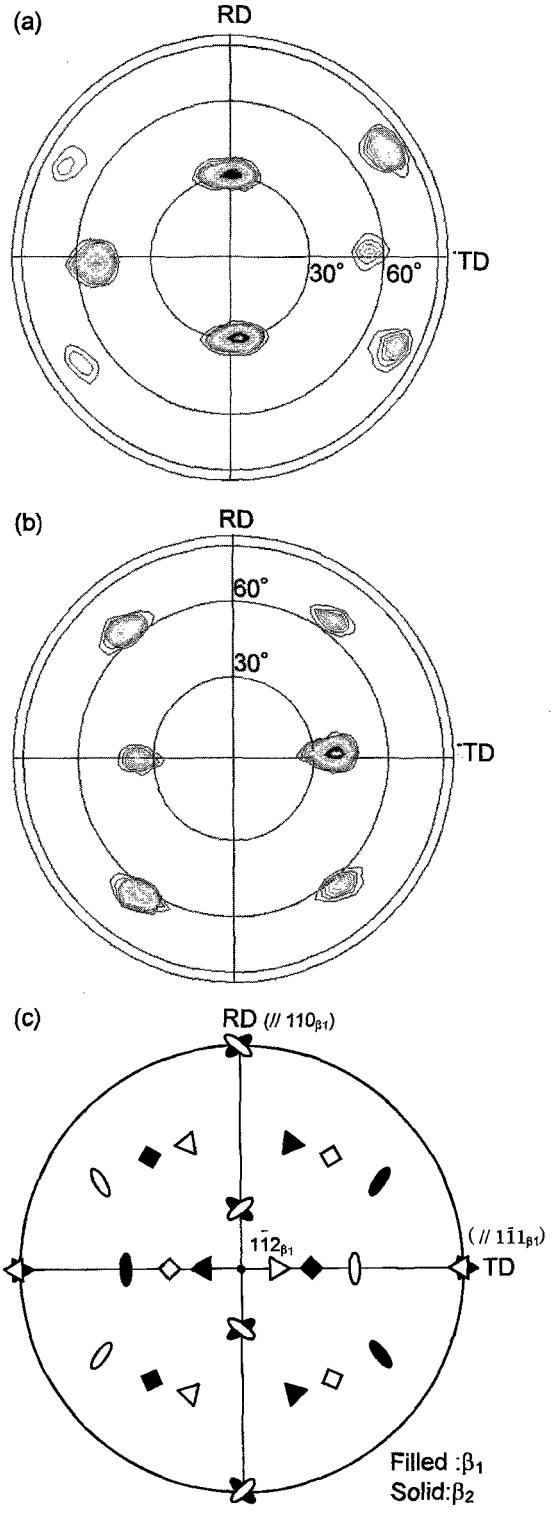

Figure 4: Pole figures of 24Nb3Al-99%-ST
(a) 110_β pole figure, Schmidt type projection
(b) 200_β pole figure, Schmidt type projection
(c) Composite stereoprojection (Wulff type) of the two variants of β ($\beta_1$and β_2)

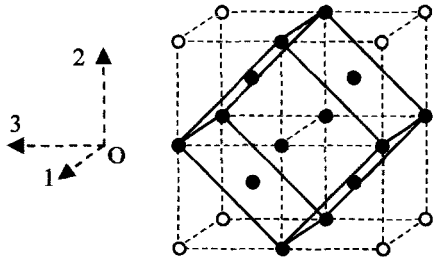

Figure 5: Lattice correspondence employed in this study Broken lines represent bcc (β) lattice. Solid lined fct is transformed into α" (C-centered orthorhombic) by the transformation. Dashed lined arrows indicates bcc lattice coordinate.

assumption of the uniform elastic constants.

$$U = -\sigma_{ij} \cdot \varepsilon^*_{ij} \quad (3)$$

The negative value of U indicates that the transformation ε_{ij}^* is assisted by the stress σ_{ij} in the total sum of components. One can realize that $-U$ is equal to the tensile strain appears along the loading direction when the calculation was conducted with a unit magnitude of an uniaxial stress σ.

The calculation was conducted only on β_1. Due to the symmetry of the system, RD and TD correspond to common crystallographic directions in both β-variants. Therefore, it is not necessary to consider the transformations in both β variants to calculate the transformation strain along RD and TD.

Table 1 shows U of each variant under RD and TD. Calculation was conducted only on β_1 (see Fig. 4(c)). Under tension along TD (// $[1\bar{1}1]_\beta$), three variants (V1, V3 and V6) have U of -0.0092 and can be stress induced. This means that when one of the three variants is induced and the specimen is entirely transformed into α'' martensite, transformation strain of 0.92% appears macroscopically along TD. As seen in Fig.1(b), the observed superelastic strain of 2.2% is the sum of 1.6% of elastic strain and 0.6% of transformation strain. Thus, the theoretically calculated transformational strain of 0.92% is in good agreement with the experimentally obtained value.

Table 1. Interaction energy U(J) of each variant

	V1	V2	V3	V4	V5	V6
tension // RD	0.0077	0.0077	0.0077	0.0077	-0.0269	0.0052
tension // TD	-0.0092	0.0122	-0.0092	0.0122	0.0122	-0.0092

On the other hand, when the tensile direction is RD (// $[110]_\beta$), only one variant (V5) has negative U of -0.0269 and can be stress induced. In this case, transformation strain along RD is 2.69%. This means that when V5 is induced and the specimen is entirely transformed into α'' of V5, transformation strain of 2.69% appears macroscopically along RD. As shown in Fig.1(a), observed superelastic strain of 4.7% is the sum of 2.2% of elastic strain and 2.5% of transformation strain. Thus, the theoretical value with the assumption that the specimen is almost single crystal is also in good agreement with the experimental value. As far as judging from the sharp peaks of intensity in pole figures, the assumption seemed to be a good approximation.

In general, the total shape change due to the martensitic transformation is consisted with the transformation strain and the lattice invariant shear strain [11]. In this study, the latter was not considered. Due to the lack of information about morphology and crystallography of α"-martensite (i.e., experimental information about habit planes, lattice invariant shear systems and orientation relationships) in this alloy composition, a precise calculation has not been conducted. The results indicate at least qualitatively that the anisotropic superelasticity in 24Nb3Al-99%-ST is due to the well developed $<110>_\beta\{112\}_\beta$ recrystallization texture.

5. CONCLUSIONS

24Nb3Al-99%-ST is consisted with equiaxed grain (averaged grain size of 74μm) of β which contains fine ω-particles (a few nm in diameter). $<110>\{112\}_\beta$ recrystallization texture is well developed in 24Nb3Al-99%-ST.

Transformation strains appear in loading directions are well explained by the transformation strain of the α"-β martensitic transformation with assuming that $<110>_\beta\{112\}_\beta$ texture is perfectly developed in the specimens. The origin of the anisotropy in superelastic properties in 24Nb3Al-99%-ST is due to the well developed $<110>_\beta\{112\}_\beta$ texture.

ACKNOWLEDGEMENTS

This work was partially supported by Furukawa Techno Material Co. Ltd., the 21st COE Program from the Ministry of Education, Culture, Sports, Science and Technology, Japan and Osawa Scientific Studies Grants Foundation. The authors would like to thank Prof. H. Ishihara, Prof. H. Funakubo and Mr. M. Suzuki in Tokyo Institute of Technology for XRD pole figure measurements.

REFERENCES

[1] H. Hosoda, Y. Fukui, T. Inamura, K. Wakashima and S. Miyazaki, *Proc of the 10th World Conf. on Titanium*, (Eds:G. Lutjering), Wiley-VCH, in press.

[2] C. R. Brooks, 'Heat Treatment, Structure and Properties of Nonferrous Alloy', ASM, Chapter 9 (1982) 329.

[3] A. R. G. Brown, D. Clark, J. Eastabrook and K. S. Jepson, *Nature*, **201**, 914 (1964).

[4] H. Hosoda, Y. Omatsu and S. Miyazaki, *Trans. MRS-J*, **26**, 235 (2001).

[5] H. Hosoda, N. Hosoda and S. Miyazaki, *Trans. MRS-J*, **26**, 243 (2001).

[6] D. L. Moffat and D. C. Larbalestier, *Metall. Trans. A*, **19A**, 1677 (1988).

[7] T. Inamura, Y. Fukui, H. Hosoda, K. Wakashima and S. Miyazaki, *Proc of the 10th World Conf. on Titanium*, (Eds:G. Lutjering), Wiley-VCH, in press.

[8] D. S. Lieberman, M. S. Wechsler and T. A. Read, *J. Appl. Phys.*, **26**, 473 (1955).

[9] M. Kato and T. Mori, *Acta Metall.*, **25**, 951 (1977).

[10] Mura, 'Micromechanics of Defects in Solids', Kluwer, Dordrecht (1982) 99.

[11] A. B. Greninger and A. R. Troiano, *Trans. AIME*, **185**, 590 (1949).

(Received October 10, 2003; Accepted March 20, 2004)